Intra-Cavity Astigmatic Mode Converting VECSEL

Nathan S. Gottesman , Michal L. Lukowski , Jason T. Meyer , Chris Hessenius, Ewan M. Wright , and Mahmoud Fallahi

Abstract—We report the design and demonstration of a vertical external cavity surface emitting laser with intra-cavity astigmatic mode converters. Using a flexible optical pumping scheme Hermite-Gaussian transverse modes were excited at the gain chip and end mirror, and Laguerre-Gaussian transverse modes were observed between the two astigmatic mode converters. Adjusting the flexible pumping scheme allowed for mode order tuning while the laser was operating.

Index Terms—Vertical external cavity surface emitting lasers, laser modes, Hermite-Gaussian beams, Laguerre-Gaussian beams, astigmatic mode converters, optical resonators.

I. INTRODUCTION

IGHER-order transverse modes have been a forefront research topic stemming from some of the initial work on lasers; however, in the past decade Laguerre-Gaussian (LG) modes have been an area of renewed intense interest due to the orbital angular momentum (OAM) these modes carry [1]. As a consequence of their structure and phase opportunities exist for many applications in areas including optical communication [2]–[5], nonlinear optics [6], [7], atom and particle trapping and manipulation [8]–[12], and imaging sciences [13]–[16].

Intra-cavity generation of LG modes was first reported in a CO_2 laser using cylindrical lenses and a spiral phase plate for mode selection [17]. Since then numerous techniques have been implemented to directly generate LG modes including: patterning defects onto cavity mirrors [18]-[20], manipulation of geometric phase using liquid crystals and meta-surfaces [21]–[24], and doughnut shaped optical pumping schemes [25], [26]. Direct generation of tunable order OAM beams has been accomplished in digital laser systems using spatial light modulators [27], [28]. Intra-cavity astigmatic mode conversion using pump power dependent thermal lensing in a solid state bounce laser has been reported [26]. First order OAM beams have also been directly generated using intra-cavity cylindrical lenses [29]. Lastly, intracavity generation of OAM modes in vertical external cavity surface emitting lasers (VECSEL) was first reported by Fresnel number manipulation [30].

Optically pumped VECSELs have been demonstrated to be reliable sources delivering high output powers over a large

Manuscript received 20 May 2022; revised 17 June 2022; accepted 22 June 2022. Date of publication 27 June 2022; date of current version 8 July 2022. This work was supported in part by the National Science Foundation Awards under Grants ECCS-1904025 and EAGER-1748606 and in part by the II-VI Foundation. (Corresponding author: Nathan S. Gottesman.)

The authors are with the Wyant College of Optical Sciences, University of Arizona, Tucson, AZ 85719 USA (e-mail: nathangottesman@email.arizona.edu; mlukowski@optics.arizona.edu; jtmeyer@email.arizona.edu; chessenius@optics.arizona.edu; ewan@optics.arizona.edu; mahmoud@optics.arizona.edu). Digital Object Identifier 10.1109/JPHOT.2022.3186684

 L_{1a} M_{1} M_{2} L_{1b} M_{2} M_{3} M_{4} M_{4} M_{5} M_{4} M_{4}

Fig. 1. Schematic of the VECSEL design for intra-cavity mode conversion with mirrors labeled M_i , cavity arm lengths labeled L_i , and mirror angles of incidence labeled θ_i . Two astigmatic mode converters (AMC) are incorporated into the design to facilitate a 2π round-trip Gouy phase shift. Mirrors M_2 and M_3 compose one AMC while mirrors M_4 and M_5 constitute a second AMC. The expected mode profiles out-coupled through each mirror are also displayed. It will be shown that the expected mode profiles out-coupled through mirrors $M_1,\,M_4,$ and M_6 are in good agreement with our experimental observations. Beam diameters are not depicted to scale. The sum of cavity arm lengths L_{1a} and L_{1b} shall be referred to as L_1 henceforth.

spectral range [31]. Open cavity design allows for wavelength tunability [32], nonlinear conversion [33], and pulse generation [34]–[36]. Recently, our group has investigated higher-order Hermite-Gaussian (HG) mode generation and astigmatic mode conversion external to the VECSEL [37]–[40]. This was done with a flexible optical pumping scheme to efficiently adjust the gain modal overlap (defined as the overlap between the gain and mode transverse profiles) resulting in controllable transverse mode tuning while the laser is operating. We then demonstrated that these modes may be converted to LG beams external to the laser cavity. In this work we propose a method to generate LG beams using intra-cavity astigmatic mode converters (AMC). A novel cavity geometry incorporating a VECSEL gain chip

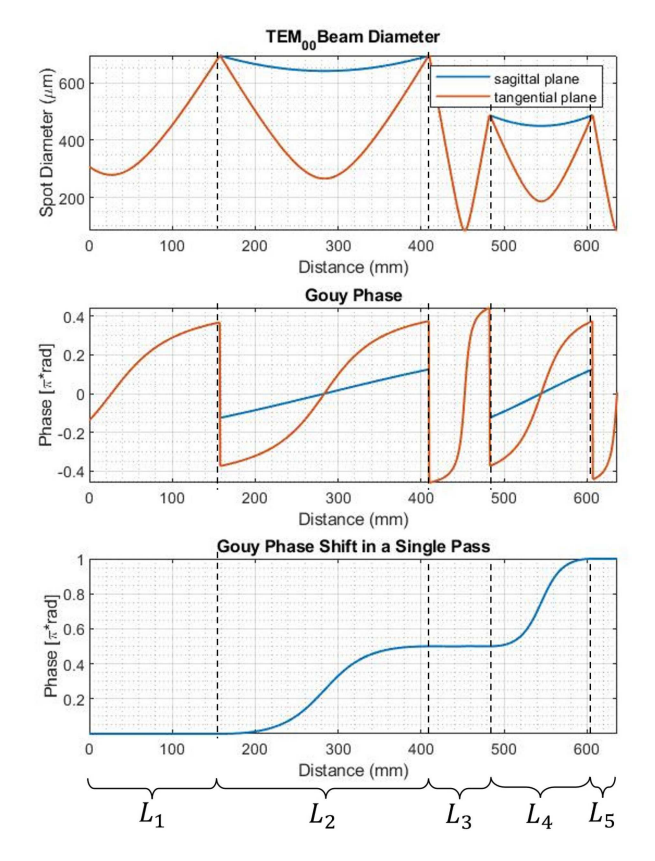


Fig. 2. ABCD matrix model of the cavity used to determine the TEM_{00} mode diameter, the Gouy phase, and the Gouy phase shift from a single pass through the cavity. The model shows that there is a π Gouy phase shift acquired in a single pass through the cavity which corresponds to a 2π round trip Gouy phase shift.

operating around 1068 nm, multiple optical pumps, and two intra-cavity AMCs were used, as shown in Fig. 1. In this cavity the mode was simultaneously a high purity HG and LG at different planes. Moreover, as we have shown in previous works [40], this laser too was capable of producing incoherent combinations of multiple transverse modes. This method for direct generation of LG beam offers a high degree of tunablity ($\ell=0$ to $\ell=16$, p=0 or p=1), while using laser mirrors with high damage thresholds as the mode converting elements. This results in a mode tunable device using common off the shelf components with high damage thresholds, which separates this method from other previous demonstrations of intra-cavity mode conversion. Experimental results and modeling are shown to be in good agreement.

II. VECSEL STRUCTURE AND FABRICATION

The VECSEL gain chip used in these experiments was a bottom emitter design, strain-compensated, InGaAs/GaAs/GaAsP multi-quantum well (MQW) heterostructure with a 25 alternating pair AlGaAs/AlAs Distributed Bragg Reflector (DBR) designed to operate at 1068 nm. The structure was composed of 12 compressively strained InGaAs QWs with GaAs barriers and GaAsP strain compensating layers. The wafer was grown using metal organic chemical vapor deposition (MOCVD) with the MQWs grown first on the GaAs substrate followed by the DBR.

TABLE I GOUY PHASE SHIFT ERROR WHEN MIRROR SEPARATIONS WERE SHORTENED BY 1 mm and Mirror AOI Made 0.1° More Acute

| Length Decreased | Mirror AOI adjusted | Gouy Phase Shift Error |
|------------------|---------------------|------------------------|
| L_1 | | > 0.001% |
| L_2 | | 0.545% |
| L_3 | | 3.638% |
| L_4 | | 0.149% |
| L_5 | | > 0.001% |
| | θ_2 | 0.285% |
| | θ_3 | 0.276% |
| | $	heta_4$ | 0.234% |
| | θ_5 | > 0.001% |

For thermal management, a chemical vapor deposition (CVD) diamond and the DBR were coated with a layer of titanium followed by a layer of gold then indium bonded together. The GaAs substrate was then selectively removed via chemical wet etch, resulting in an optically flat surface which was then AR coated with a $\lambda/4$ silica layer for the optical pump. The chip was then clamped to a water chilled copper block to remove waste heat. This fabrication process results in a system with efficient thermal management without the need for an intra-cavity heat spreader, since there is only a relatively thin DBR region between the MQWs and CVD diamond in comparison to the thickness of the GaAs substrate which was removed.

III. CAVITY DESIGN

Generally, for a laser cavity to be considered stable the supported modes must remain unchanged after a round trip. Astigmatic cavities may result in a different phase shift along the sagittal and tangential planes due to an astigmatic Gouy phase shift. External to laser cavities astigmatic focus has been manipulated with AMCs using cylindrical lens pairs and recently spherical mirrors to convert HG modes into LG modes and vice versa [41], [42]. AMCs may be understood as exploiting similarities in the decomposition of HG modes oriented at 45° and corresponding LG modes represented in the HG basis. The only difference between these two expressions is for an HG at 45° superposition terms are all in phase, while for an LG adjacent terms are out of phase by $\pi/2$. This phase factor may be physically induced by an astigmatic Gouy phase shift. This requires that in an AMC the HG mode must be oriented at 45° with respect to the planes of astigmatism for conversion to occur. If the HG mode were aligned with these planes, the mode would remain unchanged at the output of the converter.

For an astigmatic cavity, this places an additional constraint on the supported modes. For the mode to remain unchanged after one round trip the mode must be aligned with the planes of the astigmatism, unless the astigmatic Gouy phase shift is an integer multiple of 2π . This requires that two AMCs must be incorporated into the cavity design to support intra-cavity astigmatic mode conversion.

To minimize the number of surfaces in the laser cavity and improve damage threshold, fold mirrors were used to induce the Gouy phase shift instead of cylindrical lenses. The cavity which





Fig. 3. Simulated mode profile at the focus between the two AMCs (left) and at the VECSEL gain chip (right) under perfect alignment. At the VECSEL gain chip the mode profile was forced to be HG due to the gain modal overlap. This in turn forced the mode profile between the two AMCs to be LG due to the fixed Gouy phase shift relationship between the two planes.

was used in these experiments is shown diagrammatically in Fig. 1. The flexible optical pumping scheme induces an HG mode at the VECSEL gain chip oriented at 45° relative to planes of astigmatism. Mirrors M_2 and M_3 act as an AMC, transforming the HG mode into an LG mode in cavity arm L_3 . M_4 and M_5 then convert the LG mode back into an HG mode with the orthogonal orientation. On the return trip M_4 and M_5 convert the HG mode into and LG mode with opposite handedness, and finally M_2 and M_3 convert the LG mode back to an HG mode with the same orientation it initially had, satisfying the round trip condition.

IV. NUMERIC SIMULATIONS

Two simulations were developed to model intra-cavity astigmatic mode conversion. First our team analyzed the evolution of the Gouy phase shift through the cavity using the complex beam parameter and ABCD law. [43] This gave a rudimentary idea to what tolerance elements in the cavity must be held, ignoring gain modal overlap effects. We then explored how the gain profile altered these tolerances using an iterative two dimensional operator based model which simulated the transverse mode profile. As a result of the efficient heat extraction due to the CVD diamond heat spreader and the dimensions of the gain chip (\approx 5 mm \times 5 mm) we expect the transverse thermal gradient to result in a negligible thermal lensing effect for continuous wave operation, so this phenomenon was excluded from both models.

A. Complex Beam Parameter Model

Because mode conversion is induced through the Gouy phase, by tracking how it evolves through a laser cavity one may predict how the field profile should transform as it propagates. For our purposes the Gouy phase may be expressed in the useful forms given by the following:

$$\Phi = tan^{-1} \left(\frac{\lambda z}{\pi w_0^2}\right) = tan^{-1} \left(\frac{Re(q)}{Im(q)}\right)$$
$$= tan^{-1} \left(\frac{A - D}{B\sqrt{4 - (A + D)^2}}\right) \tag{1}$$

Where λ is the central wavelength, w_0 is the beam waist, z is the longitudinal position of the mode relative to the beam waist, and A, B, and D are the elements of an ABCD matrix describing a cavity in which a beam with complex beam parameter, q, is resonant.

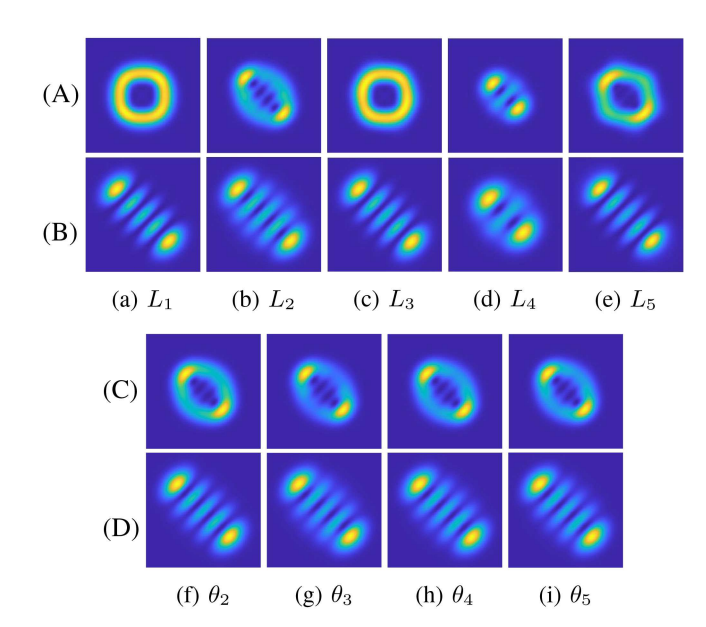


Fig. 4. Simulated mode profiles when each mirror separation, L_i , was shortened by 1 mm (columns (a)-(e)), and mode profiles when the AOI at the fold mirrors, θ_i , was decreased by 0.1° (columns (f)-(i)) at the focus in region L_3 (rows (A) and (C)) and at the VECSEL gain chip (rows (B) and (D))

Using (1), the Gouy phase of the resonant mode at any location within the cavity may be numerically calculated, as shown in Fig. 2. By slightly adjusting mirror separations or mirror angle of incidence (AOI), the change in the Gouy phase shift gives tolerances on the alignment, as summarized in Table I. From this model L_3 , which is the distance between the two AMCs and where the beam is predicted to be an LG, had the largest affect on the Gouy phase shift, while the phase shift was relatively indifferent to the end mirror M_1 and M_6 positions. Additionally, from this model the cavity stability factor given by the condition $\left|\frac{A+D}{2}\right|<1$ was extracted. The stability factor was -0.64 in both the sagittal and tangential planes which is well within the bounds of the stability condition.

B. Transverse Mode Profile Model

Flexible optical pumping schemes were used to generate higher order modes in our experiments discussed in the following section. The intent of the modelling shown here was to predict how these pumping schemes will affect the mode shape and intensity. Additionally, this model was used to show how the phase shifts given in Table I affect the resonant modes. The model used for these simulations was nearly identical to that done in reference [40], but applied to our new and significantly more complex cavity geometry. By assuming gain saturation effects to be negligible, the spatially dependent gain from the VECSEL chip may be approximated as linearly proportional to the profile of the optical pump, as seen in the following expression.

$$g(x,y) = \sum_{i} g_{i} exp \left[-\frac{(x - X_{i})^{2}}{w_{i}^{2}} - \frac{(y - Y_{i})^{2}}{w_{i}^{2}} \right]$$
 (2)

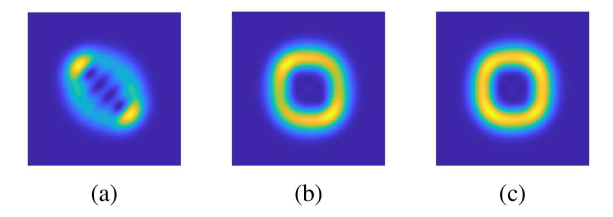


Fig. 5. Example of misalignment compensation by simulating the mode profile at the focus of arm L_3 . When L_2 was misaligned by 1 mm, the mode profile was significantly distorted (a). By intentionally shifting M_6 by 1 mm to lengthen L_5 rough compensation of the misalignment may be achieved (b). Then, by intentionally shifting M_1 by 5 mm to shorten L_1 near perfect compensation of the misalignment may be realized (c).

Where g_i is a scaling factor for the peak gain, X_i and Y_i represent the shift of the pump beams from on axis, and w_i represents the pump spot radius. The field after one round trip in the cavity may be represented by the following.

$$E_{n+1}(x,y) = e^{g(x,y) - \alpha_{\uparrow}(x,y)} \hat{K}_{\uparrow} \dots e^{g(x,y) - \alpha_{\downarrow}(x,y)} \hat{K}_{\downarrow} E_n(x,y)$$
(3)

Where $\alpha_{\uparrow|\downarrow}$ is loss from elements above or below the VECSEL chip as shown in Fig. 1, and $\hat{K}_{\uparrow|\downarrow}$ is the two dimensional generalized Huygens integral operator [44] for propagation through the elements above or below the chip and back. The initial field profile in the simulation was chosen to be the same as the gain profile to crudely approximate the portion of the spontaneous emission profile which would seed the laser. Equation (3) was applied repetitively to the field until the change from one iteration to the next became negligible.

By displacing the pumps diagonally under ideal circumstances, the mode profile at the chip was simulated to be a near perfect HG at 45° and the mode within region L_3 was found to be a near perfect LG (Fig. 3). When elements in the cavity were displaced or tilted from there ideal values; however, the stable mode profile in both regions became distorted, as seen in Fig. 4. This simulation resulted in different conclusions about the required tolerances of the design due to the inclusion of gain modal overlap effects. Most clearly, in the complex beam parameter simulation L_3 was the most sensitive parameter; however, when the gain modal overlap was included it became one of the least sensitive parameters. In both simulations L_1 was one of the most insensitive parameters. L_5 appeared to be more sensitive when gain modal overlap was included, but it was still less so than L_2 or L_4 which were the most volatile parameters. As seen in Fig. 5, slight misalignment of the cavity may be compensated using the end mirrors M_1 and M_6 to adjust L_5 to roughly correct the mode profile and L_1 to fine tune the profile. This substantially loosened the tolerances necessary for a desirable mode to be generated in region L_3 .

V. EXPERIMENTAL RESULTS

Higher order HG modes oriented at 45° with respect to the planes of astigmatism were observed out-coupled from mirrors M_1 and M_6 . These modes were orthogonal to one another,

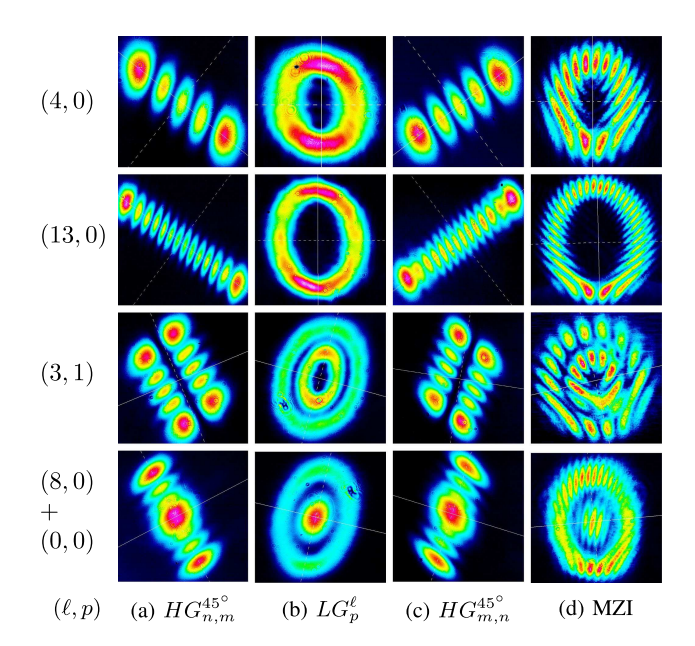


Fig. 6. HG mode profiles out-coupled through mirrors M_1 (a) and M_6 (c), the LG mode profile out-coupled through mirror M_4 (b), and the interference of the LG mode with with its parity flipped reflection from a dove prism Mach-Zehnder interferometer (MZI) (d). For the first and second row, the optical pump was displaced different distances from the optic axis, inducing tunable order, one-dimensional modes. For the third and fourth row, a second optical pump was used to excite two-dimensional modes and incoherent combinations of modes. The slight ellipticity of the LG modes suggests minor misalignment. All images were recorded using a DataRay WinCamD-LCM CMOS Beam Profiler.

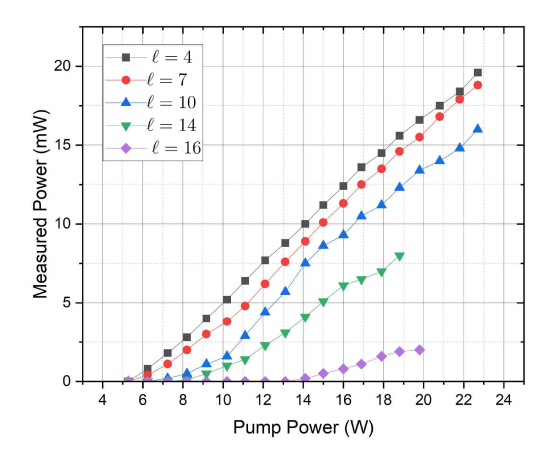


Fig. 7. The measured output power for various LG modes with one optical pump.

as predicted by our simulations. Additionally, corresponding higher order doughnut shaped modes were observed exiting mirrors M_3 and M_4 , confirming that the mode profile was indeed radially symmetric in region L_3 . To verify that the modes in L_3 were indeed vortex beams, the beam was directed into a free-space Mach-Zehnder interferometer with a dove prism in one arm. The resulting interferograms clearly displayed fringe splitting, suggesting a central phase discontinuity characteristic of LG beams. A variety of modes ranging from $\ell=0$ to $\ell=16$ were observed. This included LG_0^4 , LG_0^7 , LG_0^{10} , LG_0^{14} , LG_0^{16} characterized in Figs. 7 and 9. Incorporating a second optical pump in a similar manner to that done in [40] a LG_1^3 was

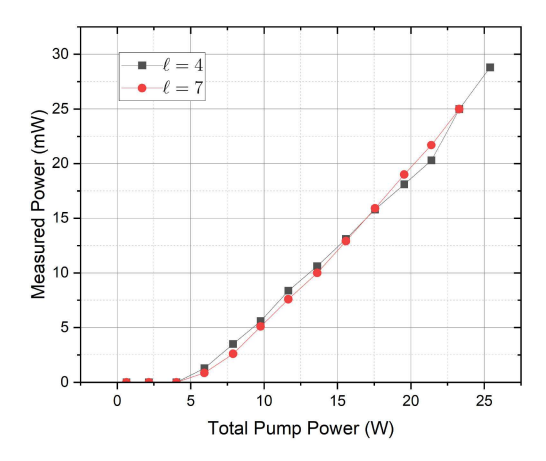


Fig. 8. The measured output power for various LG modes with two optical pumps. Total pump power is the sum of the pump power from both optical pumps. The power from each optical pump is approximately equal.

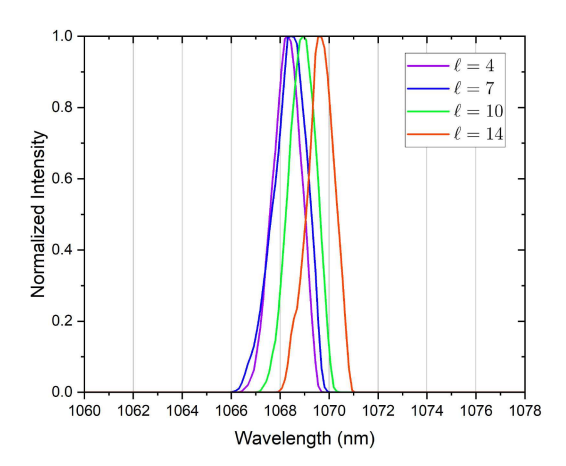


Fig. 9. The measured spectrum for various LG modes with one optical pump.

observed as well as the incoherent combination of a LG_0^8 mode and a TEM_{00} mode. A selection of these mode profiles were captured with a beam profiler and are displayed in Fig. 6 to demonstrate the broad range of high purity modes attainable with this method. Additionally, the output power characteristics of the LG modes measured from mirror M_4 are given when one optical pump (Fig. 7) and two optical pumps (Fig. 8) were used. It can be seen clearly that with mode order, there was a shift to higher threshold pump power due to a smaller gain modal overlap, resulting in less efficient optical-to-optical conversion. The incorporation of a secondary optical pump improved the gain modal overlap which resulted in a noticeable increase in slope efficiency. Lastly, the optical spectrum of a few of these modes are given in Fig. 9. There was a noticeable red shift which occurred with higher mode order. This is in good agreement with Fig. 7, as the lower optical-to-optical conversion should result in more waste heat red-shifting the spectrum. However, this thermal effect was not significant enough to noticeably reduce mode quality from off axis thermal lensing. Unlike previous demonstrations of intra-cavity mode conversion this approach has been shown to be mode tunable with high circulating powers incident on the mode converting elements, and the mode profile was independent of pump power.

VI. CONCLUSION

In summary, we have reported the design, simulation, and the clearest demonstration of intra-cavity astigmatic mode conversion in any laser system at the time of publication. A flexible optical pumping scheme was used to induce a Hermite-Gaussian mode at the VECSEL gain chip. Two pairs of fold mirrors were placed inside the cavity with particular separations and angles of incidence such that each pair induced the $\pi/2$ phase shift necessary to act as an astigmatic mode converter. It was demonstrated that the laser operates with Hermite-Gaussian and Laguerre-Gaussian mode profiles existing simultaneously at different planes in the cavity for several mode orders. Orbital angular momentum of the Laguerre-Gaussian modes was verified with Mach-Zehnder interferograms. Tuning mode order while the laser was operating was easily achievable by adjusting the location of the optical pump. With a secondary optical pump, multiple mode orders could lase concurrently. This allowed for intricate beam shaping to be done in an elegant manner, which may otherwise not be possible. Further improvements to this approach may include the optimization of the gain modal overlap with more advanced pumping schemes, improvement of the out-coupling to generate a tunable high power vortex beam light source, and lastly, miniaturization of the cavity design. Although the output powers reported here are on the order of tens of milliwatts, this is due to the high reflectivity of the cavity mirrors, resulting in strong circulating powers. These high circulating powers are enabled by the high damage threshold of the mode converting elements used in this implementation. The authors believe significantly higher efficiencies may be achieved with optimization of the out-coupling. The open cavity design lends itself to further manipulation and interaction with a high power circulating Laguerre-Gaussian beam, which may be of interest for particle trapping experiments. This cavity may be further altered for mode-locking, wavelength tuning, or nonlinear conversion, expanding the applications of this laser geometry even further.

REFERENCES

- [1] L. Allen, M. W. Beijersbergen, R. J. C. Spreeuw, and J. P. Woerdman, "Orbital angular momentum of light and the transformation of Laguerre-Gaussian laser modes," *Phys. Rev. A*, vol. 45, no. 11, pp. 8185–8189, Jun. 1992. [Online]. Available: https://link.aps.org/doi/10.1103/PhysRevA.45.8185
- [2] J. Wang et al., "Terabit free-space data transmission employing orbital angular momentum multiplexing," Nature Photon., vol. 6, no. 7, pp. 488–496, Jul. 2012. [Online]. Available: https://www.nature.com/articles/nphoton.2012.138
- [3] M. Krenn et al., "Communication with spatially modulated light through turbulent air across Vienna," New J. Phys., vol. 16, no. 11, Nov. 2014, Art. no. 113028. [Online]. Available: https://iopscience.iop.org/article/10. 1088/1367-2630/16/11/113028
- [4] A. E. Willner et al., "Optical communications using orbital angular momentum beams," Adv. Opt. Photon., vol. 7, no. 1, pp. 66–106, Mar. 2015. [Online]. Available: https://www.osapublishing.org/abstract.cfm?URI=aop-7-1-66
- [5] M. Mirhosseini et al., "High-dimensional quantum cryptography with twisted light," New J. Phys., vol. 17, no. 3, Mar. 2015, Art. no. 033033. [Online]. Available: https://iopscience.iop.org/article/10.1088/1367-2630/ 17/3/033033
- [6] K. Dholakia, N. B. Simpson, M. J. Padgett, and L. Allen, "Second-harmonic generation and the orbital angular momentum of light," *Phys. Rev. A*, vol. 54, no. 5, pp. R3742–R3745, Nov. 1996. [Online]. Available: https://link.aps.org/doi/10.1103/PhysRevA.54.R3742

- [7] J. Courtial, K. Dholakia, L. Allen, and M. J. Padgett, "Second-harmonic generation and the conservation of orbital angular momentum with high-order Laguerre-Gaussian modes," *Phys. Rev. A*, vol. 56, no. 5, pp. 4193–4196, Nov. 1997. [Online]. Available: https://link.aps.org/doi/ 10.1103/PhysRevA.56.4193
- [8] C. Alpmann, C. Schöler, and C. Denz, "Elegant Gaussian beams for enhanced optical manipulation," *Appl. Phys. Lett.*, vol. 106, no. 24, Jun. 2015, Art. no. 241102. [Online]. Available: https://aip.scitation.org/ doi/10.1063/1.4922743
- [9] K. T. Gahagan and G. A. Swartzlander, "Optical vortex trapping of particles," Opt. Lett., vol. 21, no. 11, pp. 827–829, Jun. 1996. [Online]. Available: https://www.osapublishing.org/abstract.cfm?URI=ol-21-11-827
- [10] H. He, M. E. J. Friese, N. R. Heckenberg, and H. Rubinsztein-Dunlop, "Direct observation of transfer of angular momentum to absorptive particles from a laser beam with a phase singularity," *Phys. Rev. Lett.*, vol. 75, no. 5, pp. 826–829, Jul. 1995. [Online]. Available: https://link.aps.org/doi/ 10.1103/PhysRevLett.75.826
- [11] K. C. Neuman and S. M. Block, "Optical trapping," Rev. Sci. Instrum., vol. 75, no. 9, pp. 2787–2809, Sep. 2004. [Online]. Available: https://aip. scitation.org/doi/10.1063/1.1785844
- [12] A. T. O'Neil, I. MacVicar, L. Allen, and M. J. Padgett, "Intrinsic and extrinsic nature of the orbital angular momentum of a light beam," *Phys. Rev. Lett.*, vol. 88, no. 5, Jan. 2002, Art. no. 053601. [Online]. Available: https://link.aps.org/doi/10.1103/PhysRevLett.88.053601
- [13] G. A. Swartzlander, "Peering into darkness with a vortex spatial filter," Opt. Lett., vol. 26, no. 8, pp. 497–499, May 2001. [Online]. Available: https://www.osapublishing.org/abstract.cfm?URI=ol-26-8-497
- [14] G. A. Swartzlander *et al.*, "Astronomical demonstration of an optical vortex coronagraph," *Opt. Exp.*, vol. 16, no. 14, pp. 10200–10207, 2008.
- [15] S. Fürhapter, A. Jesacher, S. Bernet, and M. Ritsch-Marte, "Spiral interferometry," *Opt. Lett.*, vol. 30, no. 15, pp. 1953–1955, Sep. 2005. [Online]. Available: https://www.osapublishing.org/abstract.cfm?URI= ol-30-15-1953
- [16] S. Fürhapter, A. Jesacher, S. Bernet, and M. Ritsch-Marte, "Spiral phase contrast imaging in microscopy," *Opt. Exp.*, vol. 13, no. 3, pp. 689–694, Feb. 2005. [Online]. Available: https://www.osapublishing.org/abstract. cfm?URI=oe-13-3-689
- [17] R. Oron, N. Davidson, A. A. Friesem, and E. Hasman, "Continuous-phase elements can improve laser beam quality," *Opt. Lett.*, vol. 25, no. 13, pp. 939–941, Aug. 2000. [Online]. Available: https://opg.optica.org/abstract.cfm?URI=ol-25-13-939
- [18] A. Ito, Y. Kozawa, and S. Sato, "Generation of hollow scalar and vector beams using a spot-defect mirror," J. Opt. Soc. Amer. A, vol. 27, no. 9, pp. 2072–2077, Sep. 2010. [Online]. Available: https://opg.optica.org/ abstract.cfm?URI=josaa-27-9-2072
- [19] S. Vyas, Y. Kozawa, and S. Sato, "Generation of a vector doughnut beam from an internal mirror He-Ne laser," Opt. Lett., vol. 39, no. 7, pp. 2080–2082, Apr. 2014. [Online]. Available: https://opg.optica.org/ abstract.cfm?URI=ol-39-7-2080
- [20] Z. Qiao et al., "Generating high-charge optical vortices directly from laser up to 288th order," Laser Photon. Rev., vol. 12, 2018, Art. no. 1800019.
- [21] D. Naidoo et al., "Controlled generation of higher-order poincaré sphere beams from a laser," Nature Photon., vol. 10, no. 5, pp. 327–332, May 2016. [Online]. Available: https://www.nature.com/articles/nphoton. 2016.37
- [22] R. Chriki et al., "Spin-controlled twisted laser beams: Intra-cavity multi-tasking geometric phase metasurfaces," Opt. Exp., vol. 26, no. 2, pp. 905–916, Jan. 2018. [Online]. Available: https://opg.optica.org/ abstract.cfm?URI=oe-26-2-905
- [23] E. Maguid et al., "Topologically controlled intracavity laser modes based on pancharatnam-berry phase," ACS Photon., vol. 5, no. 5, pp. 1817–1821, May 2018. [Online]. Available: https://pubs.acs.org/doi/ 10.1021/acsphotonics.7b01525
- [24] M. S. Seghilani et al., "Vortex laser based on III-V semiconductor metasurface: Direct generation of coherent Laguerre-Gauss modes carrying controlled orbital angular momentum," Sci. Rep., vol. 6, no. 1, Dec. 2016, Art. no. 38156. [Online]. Available: https://www.nature.com/ articles/srep38156
- [25] D. J. Kim and J. W. Kim, "Direct generation of an optical vortex beam in a single-frequency Nd: YVO_4 laser," Opt. Lett., vol. 40, no. 3, pp. 399–402, Feb. 2015. [Online]. Available: https://www.osapublishing.org/abstract. cfm?URI=ol-40-3-399
- [26] M. Okida, T. Omatsu, M. Itoh, and T. Yatagai, "Direct generation of high power Laguerre-Gaussian output from a diode-pumped Nd:YVO_4 1.3-um bounce laser," Opt. Exp., vol. 15, no. 12, 2007, Art. no. 7616. [Online]. Available: https://www.osapublishing.org/oe/abstract.cfm?uri= oe-15-12-7616

- [27] N. Zhou, J. Liu, and J. Wang, "Reconfigurable and tunable twisted light laser," Sci. Rep., vol. 8, no. 1, Dec. 2018, Art. no. 11394. [Online]. Available: https://www.nature.com/articles/s41598-018-29868-8
- [28] S. Ngcobo, I. Litvin, L. Burger, and A. Forbes, "A digital laser for on-demand laser modes," *Nature Commun.*, vol. 4, no. 1, Oct. 2013, Art. no. 2289. [Online]. Available: https://www.nature.com/articles/ ncomms3289
- [29] J. Pan, Y. Shen, Z. Wan, X. Fu, H. Zhang, and Q. Liu, "Indextunable structured-light beams from a laser with an intracavity astigmatic mode converter," *Phys. Rev. Appl.*, vol. 14, no. 4, Oct. 2020, Art. no. 044048. [Online]. Available: https://link.aps.org/doi/10.1103/PhysRevApplied.14.044048
- [30] X. Hachair, S. Barbay, T. Elsass, I. Sagnes, and R. Kuszelewicz, "Transverse spatial structure of a high fresnel number vertical external cavity surface emitting laser," *Opt. Exp.*, vol. 16, no. 13, pp. 9519–9527, Jun. 2008. [Online]. Available: https://opg.optica.org/oe/abstract.cfm?uri=oe-16-13-9519
- [31] M. Guina, A. Rantamäki, and A. Härkönen, "Optically pumped VECSELs: Review of technology and progress," *J. Phys. D: Appl. Phys.*, vol. 50, no. 38, Sep. 2017, Art. no. 383001. [Online]. Available: https://iopscience.iop.org/article/10.1088/1361-6463/aa7bfd
- [32] L. Fan *et al.*, "Extended tunability in a two-chip VECSEL," *IEEE Photon. Technol. Lett.*, vol. 19, no. 8, pp. 544–546, Apr. 2007. [Online]. Available: https://ieeexplore.ieee.org/document/4130453/
- [33] M. Lukowski, C. Hessenius, and M. Fallahi, "Widely tunable high-power two-color VECSELs for new wavelength generation," *IEEE J. Sel. Topics Quantum Electron.*, vol. 21, no. 1, pp. 432–439, Jan./Feb. 2015. [Online]. Available: https://ieeexplore.ieee.org/document/6919265
- [34] U. Keller and A. C. Tropper, "Passively modelocked surface-emitting semiconductor lasers," *Phys. Rep.*, vol. 429, no. 2, pp. 67–120, Jun. 2006. [Online]. Available: https://linkinghub.elsevier.com/retrieve/ pii/S037015730600127X
- [35] J. T. Meyer, M. L. Lukowski, C. Hessenius, E. M. Wright, and M. Fallahi, "High peak power, sub-ps green emission in a passively mode locked W-cavity VECSEL," *Opt. Exp.*, vol. 28, no. 4, pp. 5794–5800, Feb. 2020. [Online]. Available: https://www.osapublishing.org/abstract.cfm?URI=oe-28-4-5794
- [36] J. T. Meyer, M. L. Lukowski, C. Hessenius, E. M. Wright, and M. Fallahi, "All-intracavity fourth harmonic generation in a passively mode locked VECSEL for ultrafast UV emission," *Opt. Commun.*, Jul. 2021, Art. no. 127255. [Online]. Available: https://linkinghub.elsevier.com/retrieve/pii/S0030401821005046
- [37] M. L. Lukowski, J. T. Meyer, C. Hessenius, E. M. Wright, and M. Fallahi, "Generation of high-power spatially structured beams using vertical external cavity surface emitting lasers," *Opt. Exp.*, vol. 25, no. 21, pp. 25504–25514, Oct. 2017. [Online]. Available: https://www.osapublishing.org/abstract.cfm?URI=oe-25-21-25504
- [38] M. L. Lukowski, C. Hessenius, J. T. Meyer, E. M. Wright, and M. Fallahi, "High power two-color orbital angular momentum beam generation using vertical external cavity surface emitting lasers," *Appl. Phys. Lett.*, vol. 112, no. 4, Jan. 2018, Art. no. 041108. [Online]. Available: https://aip.scitation. org/doi/10.1063/1.5009090
- [39] M. L. Lukowski, J. T. Meyer, C. Hessenius, E. M. Wright, and M. Fallahi, "Watt-level high order Hermite-Gaussian and Laguerre-Gaussian beams from vertical external cavity surface emitting lasers," in *Proc. IEEE Int. Semicond. Laser Conf.*, 2018, pp. 1–2. [Online]. Available: https://ieeexplore.ieee.org/document/8516238/
- [40] M. L. Lukowski, J. T. Meyer, C. Hessenius, E. M. Wright, and M. Fallahi, "High-power higher order Hermite-Gaussian and Laguerre-Gaussian beams from vertical external cavity surface emitting lasers," *IEEE J. Sel. Topics Quantum Electron.*, vol. 25, no. 6, Nov./Dec. 2019, Art. no. 1500406. [Online]. Available: https://ieeexplore.ieee.org/document/8675371/
- [41] M. W. Beijersbergen and L. Allen, "Astigmatic laser mode converters and transfer of orbital angular momentum," *Opt. Commun.*, vol. 96, no. 1, pp. 123–132, 1993.
- [42] R. Uren, S. Beecher, C. R. Smith, and W. A. Clarkson, "Method for generating high purity Laguerre-Gaussian vortex modes," *IEEE J. Quantum Electron.*, vol. 55, no. 5, Oct. 2019, Art. no. 1700109. [Online]. Available: https://ieeexplore.ieee.org/document/8772174/
- [43] H. Kogelnik and T. Li, "Laser beams and resonators," *Proc. IEEE*, vol. 54, no. 10, pp. 1312–1329, Oct. 1966. [Online]. Available: https://ieeexplore.ieee.org/document/1447049/
- [44] A. E. Siegman, Lasers. Mill Valley, CA, USA: Univ. Science Books, 1986.